Scaling of Cavitation Damage

D. R. Stinebring,* R. E. A. Arndt,† and J. W. Holl‡
Pennsylvania State University, State College, Pa.

This investigation has focused on the initial stages of cavitation erosion using a ductile material in a flowing system employing water as the working fluid. The test models were 0.25-in. (0.635-cm)-diam zero-caliber ogives made of pure annealed aluminum. The damage was in the form of small round depressions in the model surface. In the formation of these pits, there was no material removal. For a range of velocities from 49 to 195 fps (14.9 to 59.3 m/sec), the pitting rate increased by approximately the sixth power of velocity. The average volume of the cavitation damage pits increased by the fifth power of velocity. A relationship between the volume of a pit and the absorbed bubble collapse energy was developed. The rate of total bubble collapse energy absorbed by the model then increases by the eleventh power of velocity. A plot of the distribution of absorbed collapse energies was generated for three flow conditions. The effect of cavitation number and air content of the working fluid were also major areas of investigation. A high-speed motion-picture study of cavity dynamics was undertaken to understand better some of the processes involved in cavitation damage. Lastly, the results of this study were compared with those of previous investigations of cavitation erosion.

I. Introduction

THE destructive action caused by cavitation has been a practical problem for a long time. Erosion of ship propellers and hydraulic turbine blades can cause a loss in performance, leading to eventual costly maintenance or replacement of the damaged part. Ship hull appendages, diesel cylinder liners, hydrofoils, valves, and even the sluice gates on hydroelectric power dams are subject to cavitation damage. The damage is caused by the collapse of small vaporous cavities as they travel into a high-pressure region. Upon collapse, enormous pressures are generated. If the cavitation bubble collapse occurs near a boundary, damage can occur.

Accurate prediction of cavitation damage is very difficult. After nearly 100 years of research in cavitation, the problem of scaling model damage data to prototype conditions is unsolved. It is not that there has been a lack of study in this area, for the literature dealing with this subject is voluminous to say the least. Rather, the lack of success is because cavitation damage involves both fluid and solid mechanics and thus is inherently difficult.

The attack caused by the collapse of one cavitation bubble occurs over a very small area (on the order of hundredths of a square millimeter) and in a very short time interval (measured in microseconds). Both the hydrodynamic aspects of the cavity flow and the material response to the impact loading caused by the cavity collapse must be considered. The problem is complicated further by possible interactions between cavitation and corrosion.

This investigation has focused on the initial stages of cavitation erosion using a ductile material, namely pure aluminum, in a flowing system employing water as the working fluid. It is not a study of the erosion of aluminum, but the aluminum was used as a device for recording the intensity of each cavitation bubble collapse. The damage to the surface of a ductile material is initially in the form of small identations in which no material is removed. The name most often given to this regime of cavitation damage is the "incubation zone" as named by Thiruvengadam.[1] It has been shown[2] that, in the incubation zone, each indentation is produced by the collapse of one cavitation bubble. There, is then, a one-to-one correspondence between the bubble collapse and the damage thereby produced.

If the duration of exposure to cavitation is increased past the incubation zone, weight loss will occur. In most previous investigations, cavitation damage has been assessed by the rate of weight loss. However, in the weight loss zone, there is no one-to-one correspondence between damage and a single bubble collapse, as in the incubation zone. In the weight loss zone, damage can be caused by hydrodynamic blows of many bubbles. Furthermore, the problem is complicated in this zone by possible interactions between cavitation erosion and corrosion. Because of the aforementioned complexities of the weight loss zone, it was decided that this investigation should be conducted in the incubation zone, where there is a one-to-one correspondence between cavitation damage and the collapse of a single bubble.

This research was concerned with the hydrodynamic aspects of cavitation damage and the effect of alteration of the flow parameters upon the damage to a model. Many cavitation damage studies have been conducted in nonflow systems employing a vibratory apparatus. However, this study was conducted in a flowing system in order to approximate real engineering situations more closely. The major goal of the investigation was to observe the effect of velocity, cavity length, and air content on the rate of cavitation damage in the incubation zone, with velocity as the primary variable. It has been shown by Knapp[2] that the rate of cavitation damage in the form of small identations in a model's surface increases by the sixth power of velocity. Knapp's study was conducted over a relatively narrow velocity range (~18 to 30.5 m/sec). A much larger range of velocities (14.9 to 59.3 m/sec) was employed for this investigation.

The number of pits produced on a model's surface can be used as a measure of cavitation damage. However, the size of the individual pits also should be considered. The volume of each indentation in the surface is proportional to the cavitation bubble collapse energy absorbed by the model. By recording both numbers and volumes of the identations, a relative measure of the total collapse energy absorbed is known. The change in the total collapse energy per second with velocity was an area of investigation.

It was necessary to relate the volume of each cavitation damage pit to the energy of formation. A hardness test that

Presented as Paper 77-317 at the AIAA 13th Annual Meeting and Technical Display Incorporating the Forum on the Future of Air Transportation; submitted Jan. 21, 1977; revision received March 18, 1977.

Index categories: Hydrodynamics; Multiphase Flows.

*Research Assistant, Applied Research Laboratory. Student Member AIAA.

†Associate Professor, Applied Research Laboratory. Member AIAA.

‡Professor, Applied Research Laboratory. Associate Fellow AIAA.

measures the surface hardness of the model material at a high strain rate, termed a dynamic hardness test, was devised for this purpose. Most hardness tests are conducted at nearly a zero strain rate, but in the formation of a cavitation pit the strain rates involved are very high. To account for this fact, a surface hardness measurement at a high strain rate is required. To approximate this condition, the dynamic hardness test was devised. From these measurements of the dynamic hardness of the 1100-0 aluminum, an approximate measure of the energy required to form a given pit was obtained.

Knowing the rate of pit production, the average pit volume for a given flow condition, and the dynamic hardness of the model material, a scaling relationship between the velocity and cavitation bubble collapse energy absorbed was developed. This was probably the most important phase of the investigation, since it involved a scaling of the total damage (and damage potential energy) on a one-to-one correspondence with the bubble collapse.

Since the material utilized as the damage probe was so very soft, even a cavitation bubble with relatively low collapse energy will cause an indentation in the surface. The observation of a wide range of energies is then possible. The collapse energy distribution for the same flow conditions will remain unchanged irrespective of the test body material; only the response of various test materials to the applied hydrodynamic forces will change. This itself is most helpful in an understanding of the processes involved in the study of cavitation damage.

II. Experimental Program

Water-Tunnel Test Procedures

The water-tunnel testing was divided into three main phases. The initial phase was conducted in the 30.5-cm cavitation tunnel, whereas phases II and III were in the 3.8-cm ultra-high-speed cavitation tunnel. The 30.5-cm tunnel has a maximum velocity in the test section of about 25 m/sec, whereas the 3.8-cm tunnel has a maximum velocity of over 92 m/sec. Both facilities are a part of the Garfield Thomas Water Tunnel of the Applied Research Laboratory complex at The Pennsylvania State University. The models utilized in this investigation were 0.635-cm-diam zero-caliber ogives with the area subject to damage made of 1100-0 aluminum.

The phase I tests in the 30.5-cm tunnel were conducted as a preliminary investigation prior to testing in the high-speed tunnel. A few of the area of interest in conducting this phase of investigation were as follows:

1) How long should a model be run to obtain a sufficient damage sample for analysis?

2) Does the duration of the test affect the rate at which pits are produced?

3) In what form would the damage be (large pits, small pits, deep, shallow, etc.)?

The main phases of the investigation, phases II and III, were conducted in the 3.8-cm cavitation tunnel. All of the scaling relationships were developed in this tunnel. The phase II tests were run at high air contents, whereas phase III was conducted at lower gas contents. High-speed movies of the cavity behavior also were shot in this tunnel.

For phase II and III, a wide range of velocities and cavity lengths was tested to observe the effect upon the rate of damage production. The velocity was varied from 14.9 to 59.3 m/sec in intervals of 7.6 m/sec. The cavity length was expressed in nondimensional form by dividing the length of the cavity by the model diameter (L/D). The range of dimensionless cavity lengths was 1.0 to 6.0. This corresponds to a change in the cavitation number (σ) from 0.625 to 0.316, where σ is defined as

$$\sigma = (P_\infty - P_c) / \tfrac{1}{2}\rho_L V_\infty^2$$

where

P_∞ = freestream static pressure
P_c = cavity pressure
ρ_L = mass density of the liquid
V_∞ = freestream velocity

The air content of the water was varied from 10 to 20 ppm on a molar basis to test its effect upon the damage. For each test, a new model was machined and annealed to retain a permanent record of the accumulated damage.

An important requirement had to be met in order for the analysis to be valid. The damage rate for a given flow condition had to be independent of the test duration. At first this would seem logical, since, if the flow conditions did not change, it would be expected that there would be twice as many pits for a 2-hr test as for a 1-hr test. This probably would not be the case, though, if the number density of pits became so great as to overlap. Annealed pure aluminum is a mterial susceptible to work-hardening. If a bubble collapses and produces an indentation, the surface is deformed and work-hardened. If another bubble collapses in the same area with the same energy, it will "see" a greater surface hardness because of the work-hardening. The resulting deformation then will be less for the same impact energy. Care was taken, by a suitable choice of test duration, to insure that the pits were in sufficient density for ease of analysis but not so close as to overlap. A special test was conducted during phase I to determine whether, in fact, the damage rate was independent of test duration.

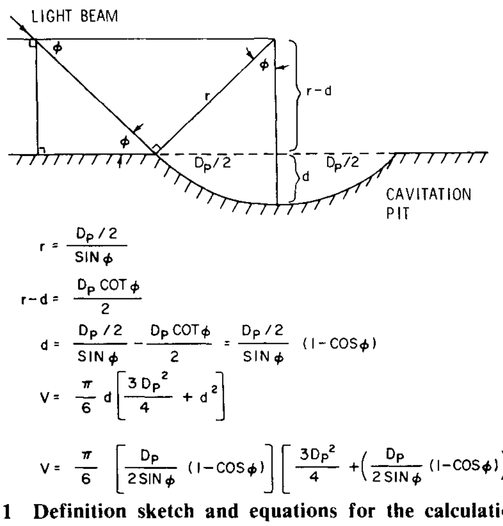

$$r = \frac{D_p/2}{\sin\phi}$$

$$r - d = \frac{D_p \cot\phi}{2}$$

$$d = \frac{D_p/2}{\sin\phi} - \frac{D_p\cot\phi}{2} = \frac{D_p/2}{\sin\phi}(1-\cos\phi)$$

$$V = \frac{\pi}{6} d\left[\frac{3D_p^2}{4} + d^2\right]$$

$$V = \frac{\pi}{6}\left[\frac{D_p}{2\sin\phi}(1-\cos\phi)\right]\left[\frac{3D_p^2}{4} + \left(\frac{D_p}{2\sin\phi}(1-\cos\phi)\right)^2\right]$$

Fig. 1 Definition sketch and equations for the calculation of pit volumes.

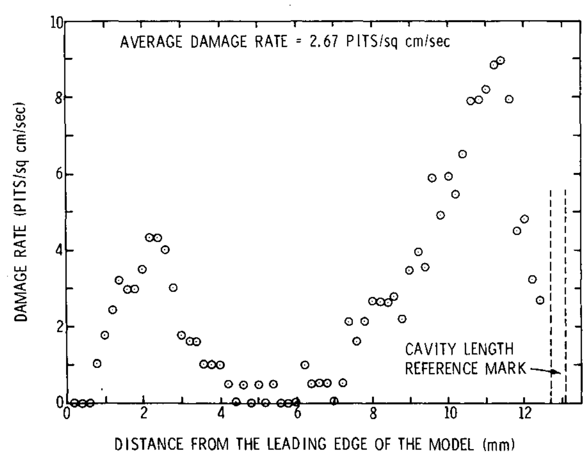

Fig. 2 Plot of the damage rate distribution along a phase I test model (model 1, V_∞ = 21.3 m/sec, L/D = 2.0, and 30-min test duration).

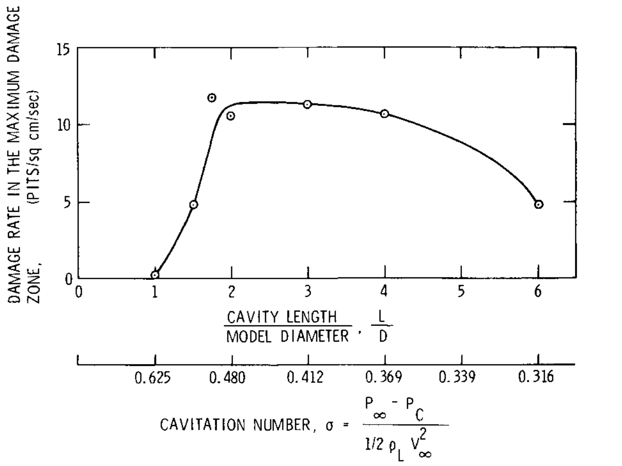

Fig. 3 Damage rate in the maximum damage zone vs dimensionless gravity length and cavitation number (phase III models, $V_\infty = 38$ m/sec, and air content of 10 ppm).

A further study was conducted involving the dynamics of the developed cavity on the test body with the use of high-speed cinematography. Past studies have shown that cavity motion is very unsteady for developed cavities. Thus it was decided that a high-speed study of cavity behavior could enhance the understanding of the cavitation erosion mechanism. A Redlake Hycam and an EG and G type 501 Strobe were used for photographing the cavity. A framing rate of 5000 pictures/sec proved adequate for observation of the processes involved. For all movies, transmitted lighting was used; the camera and strobe unit were on opposite sides of the object to be photographed.

Analysis of Damage

The main instrument utilized in the analysis of the damage was an American Optical Microstar series light microscope. A Bausch and Lomb illuminator provided a bright collimated light source for viewing the shallow cavitation pits. The illuminator was placed at a very low lighting angle for best contour distinction.

The damage to the test models was measured along a narrow strip parallel to the model's axis of symmetry from the leading edge to a point where the damage approached zero. This strip was divided into equal reference areas, with the number of pits in each reference area along the surface recorded. Thus, at each axial station along the model, there would be a data point indicating the number of pits in the sample area. The pit distribution along the model could be converted into a damage rate distribution by calculating the number of pits per square centimeter at any point and dividing by the total test duration. The average damage rate for any area on the model, such as the maximum damage zone, then could be calculated. In this analysis, magnifications of 100 and 150× were used, and pit diameters greater than or equal to 0.01 mm were recorded.

As stated previously, one aim of this investigation was the development of a scaling relationship for the bubble collapse energy with velocity. To accomplish this, the volumes of a representative number of cavitation pits for a given model had to be measured and the average computed. The determination of the pit volumes at first proved to present a problem. The vast majority of the identations were on the order of 0.05 mm diam, with some as small as 0.01 mm. In addition, the pits tended to be very shallow. Measuring the pit depths from parallax measurements proved difficult because the pits had such an indistinct boundary, and reference points for the parallax measurements were difficult to observe.

Table 1 Test data for phase II and III tests

Model Number	Velocity (m/sec)	L/D	Pitting Density in the Maximum Damage Zone (pits/cm^2)	Damage Rate in the Maximum Damage Zone (pits/cm^2/sec)	Air Content (ppm)	Test Duration (minutes)	Test Phase
10	38.22	1	----	----	16.5	10	II
11	23.26	1	----	----	----	45	II
12	43.59	1	----	----	16.7	3	II
13	30.87	1	----	----	19.3	20	II
15	30.60	2	3294	2.740	19.9	20	II
16	38.31	2	6066	5.050	17.3	20	II
17	42.82	2	2973	16.430	20.0	3	II
18	30.02	3	2497	2.770	19.0	15	II
19	38.19	3	4140	6.898	18.5	10	II
20	22.95	3	1102	0.306	20.3	60	II
21	42.64	3	2518	20.930	19.7	2	II
22	30.11	4	2546	2.830	18.0	15	II
25	42.89	4	2206	18.380	16.7	2	II
26	23.29	2	1273	0.423	20.6	50	II
27	37.37	1.75	7033	11.720	10.3	10	III
29	37.22	1.5	4368	4.850	7.7	15	III
30	37.37	1	409	0.273	7.9	25	III
31	29.87	1	1453	0.969	7.5	25	III
32	23.16	2	1439	0.800	10.7	30	III
33	23.16	2	4027	2.230	8.1	30	III
34	23.20	2	2478	1.380	7.63	30	III
35	37.12	2	3396	10.570	11.7	5.5	III
37	37.98	3	4033	11.210	9.5	6	III
38	30.11	3	2712	2.98	9.85	9	III
39	43.65	3	2832	31.47	13.40	1.5	III
41	49.26	3	3881	126.00	8.30	0.47	III
42	38.22	4	6353	10.59	9.85	10	III
43	43.43	4	4035	44.80	9.84	1.5	III
44	29.84	3	4712	4.62	11.20	17	III
45	30.51	4	4267	3.56	8.40	20	III
46	49.98	4	4753	83.90	8.50	0.88	III
51	14.87	2	1903	0.151	6.65	210	III
52	36.82	3	5390	17.96	7.08	5	III
55	22.52	3	3996	1.903	7.62	35	III
57	36.45	6	4263	4.735	7.98	15	III
82	51.33	2	3746	124.80	9.09	0.5	III
83	59.28	3	2105	272.00	11.50	0.08	III

It was noticed in the counting of the damage pits through the microscope that the lighting angle for viewing was critical. If the angle was too high, there was no shadowing and the pits were not visible. This effect was used in the calculation of the volumes of the identations.

As an approximation, the damage pits were assumed to be spherical segments. A collimated light beam illuminated the pit, as shown in Fig. 1. The angle at which the light strikes the surface was adjustable. When the light beam is tangent to the side of the pit at the rim, there will be no shadow.

The individual pit was viewed with the microscope at 100×. The angle of the light beam was raised until there is no shadow within the pit. By knowing this lighting angle, the pit diameter and the approximation to a spherical segment, the pit volume can be calculated. A large number of pits where chosen randomly and the volumes measured using this procedure. An average pit volume for a given model then was obtained. Pit volume measurements were made for those models tested at a dimensionless cavity length of 2.0 at velocities of 30.1, 38.0, and 49.3 m/sec.

Determination of Dynamic Hardness

The dynamic hardness test was used to obtain a relationship between the volume of a cavitation pit and the energy required to form it. The apparatus constructed for the dynamic hardness test was fairly simple. An electromagnet held the indenter, which was a hardened steel ball, a specified distance above the annealed aluminum sample on which the test was to be performed. When the current to the electromagnet was shut off, the indenter would fall, and a strobe light flashing at the rate of 60 flashes/sec illuminated the ball throughout its trajectory.

A camera shutter was opened when the ball started to fall. The trajectory then was recorded at intervals due to the strobe flash. The ball, after striking the sample, rebounded from the surface. A graduated rule next to the indenter trajectory also was recorded in the multiple exposure. The camera shutter was closed after the motion had stopped. The maximum point at which the images of the ball overlapped after impact is the rebound height.

After each drop test, the diameter of the pit in the sample surface was measured to the nearest 0.005 mm with a microscope. By knowing the drop height, rebound height, ball

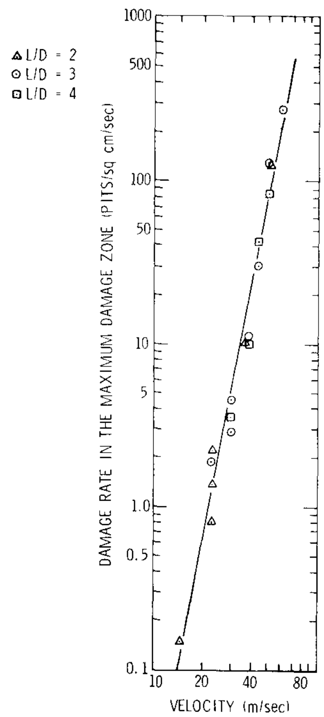

Fig. 4 Damage rate in the maximum damage zone vs velocity for phase III models (air content of 10 ppm).

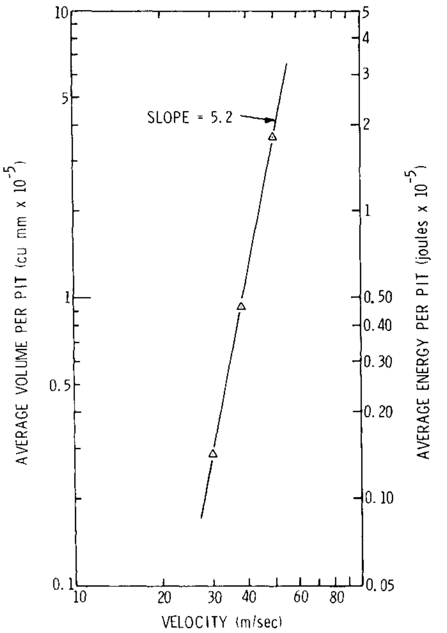

Fig. 5 Average pit volume (average energy per pit re a dynamic hardness of 0.5 J/mm^3) vs velocity (L/D=3.0 and an air content of 10 ppm).

mass, ball diameter, and the diameter of the pit formed by the ball, the energy per unit pit-volume was calculated. This energy per unit volume is the dynamic hardness. Descriptions of similar devices for calculating the dynamic hardness can be found in Ref. 3.

III. Discussion of Results

General Observations

As stated previously, phase I was conducted as preliminary tests prior to the main phases of testing. The general areas of interest were test duration, test procedures, and appearance of the cavitation damage.

In Fig. 2, it can be seen that, for model 1, the damage starts from zero at the leading edge, reaches a small peak at about 2.5 mm downstream, decreases to nearly zero, and reaches a larger peak 11.7 mm from the leading edge. The larger peak corresponds to the point of cavity closure on the model, i.e., $L/D \cong 2.0$ for this model. Beyond this point, there is almost no damage.

It was found that, at 21.3 m/sec and L/D of 2.0, significant damage was observed after only 15 min of testing with a 30-min run, providing a good damage sample. With longer test durations, namely 1 hr, the pits became so closely packed that overlapping commenced. The average damage rate was found to be independent of test duration if the pits did not overlap.

The indentations caused by the cavitation had a wide range of sizes. The largest were 0.15 mm diam, the smallest about 0.01 mm across, with the majority of the pits being less than 0.025 mm diam. There was no material removed from the surface during the formation of these pits, since the machine tool marks from machining the models were visible over the surface of the indentations. If any material had been removed, there would be a break in the tool marks on the body.

Another unusual effect observed during phase I was pitting near the leading edge of the models. According to classical theories of cavitation damage, there should be no damage in this area. It was felt that the unsteady nature of the cavity behavior could have a bearing on the problem. It was for this reason that the high-speed photographic study of cavity dynamics was conducted.

For photographing the cavity, a framing rate of 5000 pictures/sec proved adequate. The cavity cycle begins with a relatively long period, during which the cavity remains "steady." The cavity then breaks off at the leading edge and rolls back over the model, usually in two separate segments. Small vortices usually connect the fragments as they travel downstream. The cavity breaks off because of a re-entrant jet moving through the cavity and striking the leading edge. For very short and very long cavity lengths, there was no cycling of the cavity. In the first case, there is no well-denfined cavity. In the second, the re-entrant jet does not have the momentum to reach the leading edge of the cavity and cause it to break off.

It is felt that the force of the re-entrant jet striking the leading edge of the cavity wall could cause a substantial short-term pressure rise. This pressure rise, in turn, could cause the collapse of any tiny cavitation bubbles in the area and produce damage. No damage was observed near the leading edge of the models for those tested at very short cavity lengths. Only one model was tested at a long cavity length for which no cavity cycling occurred. In this case no damage was observed near the leading edge also.

Scaling Considerations

Effect of cavity length on the pitting rate

The test parameters and results of the primary phases of testing, phase II and III, are given in Table 1. During phase III, a study of the effect of cavity length on the damage was conducted. The tests were conducted over a wide range of cavity lengths at a velocity of approximately 38 m/sec and an air content of 10 ppm. Seven cavity lengths corresponding to dimensionless cavity lengths of 1.0, 1.5, 1.75, 2.0, 3.0, 4.0, and 6.0 were tested. The results are shown in Fig. 3.

The production of damage is very low for the shorter cavity lengths, increases to a peak, and then decreases for the longest cavity tested. At a dimensionless cavity length of unity, there is almost no damage to the surface. This concurs with results obtained for this cavity length at other velocities during phase II and III tests. The flow over a zero-caliber ogive is a separated flow. For very short cavities, the cavitation bubbles grow and collapse in the freestream away from the model. At longer cavity lengths, the downstream portion of the cavity is attached to the model. This allows the bubbles to collapse close to the surface and increase the damage capability.

Effect of velocity on the pitting rate

The main objective of the investigation was to observe if the damage rate increased by a constant power of velocity for a wide range of velocities. If this were true, the data should plot as a straight line on log-log paper, with the slope of the graph equal to the velocity exponent. The results are shown in Fig. 4., with slope of the curve nearly equal to 6. The damage rate in the maximum damage zone then scales by nearly the sixth power of velocity. The data for dimensionless cavity lengths of 2.0, 3.0, and 4.0 are plotted on the same graph. This was

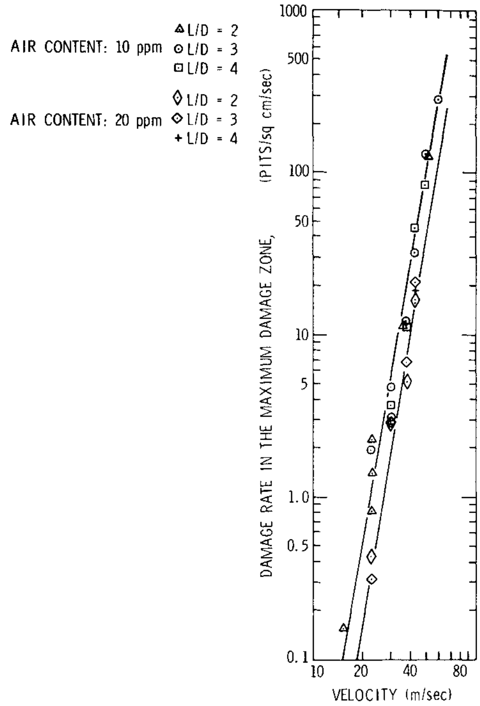

Fig. 7 Effect of air content on the damage rate in the maximum damage zone.

done because it was found that the damage rate at any one velocity does not vary appreciably for those cavity lengths tested, as shown in Fig. 3. Plotting the values for the three cavity lengths provided a larger sampling in the generation of the velocity scaling curve.

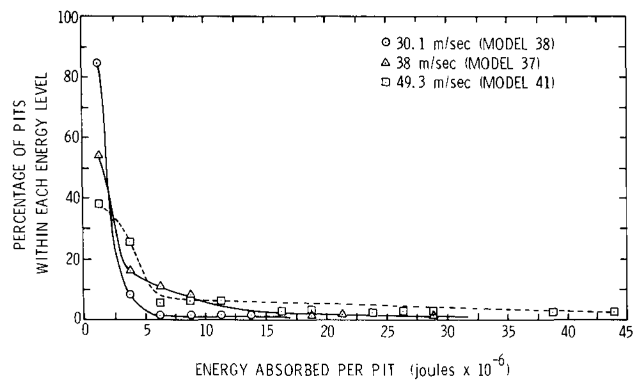

Fig. 6 Energy probability density distribution for test velocities of 30.1, 38.0, and 49.3 m/sec ($L/D = 3.0$ and an air content of 10 ppm).

Effect of velocity on the bubble collapse energy

As stated previously, the volume of a pit is a measure of the energy required to form it. The dynamic hardness test was performed to relate the volume of a cavitation pit to the cavitation bubble collapse energy absorbed by the model. A wide range of indenter drop heights (20 to 100 cm) was tested with two indenters (0.125 and 0.625 g). For the entire range of tests, the scatter in the data was quite small, with the average dynamic hardness equal to 0.50 J/mm^3.

The volumes of a random sampling of pits were computed for models run at velocities of 30.1, 38.0, and 49.3 m/sec for a dimensionless cavity length of 3.0. The velocity had a marked effect on the average volume. The average pit volume and average collapse energy absorbed are plotted in Fig. 5 as a function of velocity. The slope of the curve on log-log paper shows that the average volume and average collapse energy absorbed increase by the fifth power of velocity. Since the pitting rate increases to the sixth power of velocity and the average collapse energy to the fifth, the total cavitation bubble collapse energy absorbed per unit area per second increases to the eleventh power.

The pit volume is a measure of the collapse energy absorbed; a plot of the pit volume distribution for a given flow condition is then a plot of the distribution of absorbed bubble collapse energy. Figure 6 is a very rough plot of the envelopes of the pit volume distribution graphs, accounting for the total number of pits in each sample. The plot was generated as follows. The abscissa was divided into equal absorbed bubble collapse energy levels of 2.5×10^{-6} J or a change in pit volume of 5×10^{-6} mm^3 between each level. The relationship between the pit volume and collapse energy absorbed corresponds to 0.5 J/mm^3, which was the result from the dynamic hardness test. The percentage of collapse energies absorbed within each level then was plotted. This was done for the three velocities tested. Even with such a small statistical sample, the relative partition of the absorbed

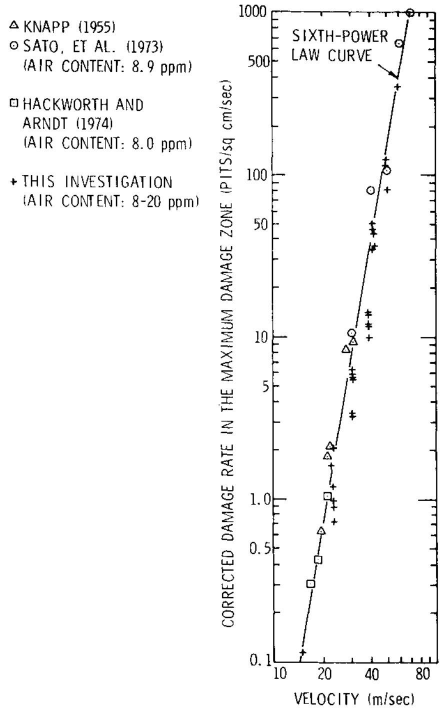

Fig. 8 Damage rate in the maximum damage zone vs velocity for investigations of cavitation damage in which there is no weight loss; corrected for air content.

bubble collapse energy is seen for each velocity. For the lowest velocity, there are large number of bubbles collapsing with relatively little damage to the boundary. As the velocity increases, there is a greater percentage of pits formed by a much higher collapse energy.

Effect of air content on the pitting rate

From a study of the literature, it appears that the air content was not a major variable in most investigations. During this investigation, a significant effect of air content on the damage rate has been observed with a comparison of the data from phase II and III. The effect of air content can be seen best in Fig. 7. The upper curve is the damage rate in the maximum damage zone as a function of velocity for an air content of approximately 10 ppm, whereas the lower curve corresponds to data at 20 ppm. For a doubling of the air content, the damage rate is cut approximately in half. One model was tested at a lower air content, namely 7 ppm, to observe if the damage rate would increase further. The model was tested at a velocity of approximately 38 m/sec and a dimensionless cavity length of 3.0. The damage rate in the maximum damage zone was 48.2 pits/cm^2/sec for an air content of 7 ppm and 37.1 pits/cm^2/sec for a model run at 10 ppm at the same velocity and cavity length. This shows that the damage rate does increase further for a decrease in air content. This change in damage production due to variations in air content could be one source of scatter of data in the literature. Although no quantitative data was obtained, because of the time element involved, the pits at the lower air content appeared to be larger than their counterparts at the higher air contents.

Comparison of Results with Other Investigations

A comparison was made between four investigations of cavitation damage in the incubation zone using aluminum as a test body. Data from Knapp,[2] Hackworth and Arndt,[4] Sato et al.,[5] and this investigation were compared. All investigations measured the damage rate, in the form of pits per second per unit area, on a pure annealed aluminum model. Sato used type A. A. 1080, Alcoa BC 1 S aluminum, 99.8% pure, whereas the others used 1100 aluminum, 99% pure. Knapp employed a 5.08-cm-diam hemispherical-nosed body, whereas Sato's test body had a 1-cm hemispherical nose. Hackworth and Arndt measured the damage downstream of a 0.635-cm-high step mismatch, and this investigation a 0.635-cm-diam zero-caliber ogive. A range of cavity lengths and air contents also was contained in the data.

Good agreement in the data was found for the investigations. It was decided to correct all data to one air content. This was done using the hyperbolic relationship found from the tests conducted during this investigation. The results are shown in Fig. 8. For such a wide variation of model size and geometry, the data corrected only for air content show remarkable agreement. From this comparison, it would seem that the variation of the velocity overrides the differences with flow configurations and σ.

IV. Summary

The damage in its initial stages was in the form of small indentations in the surface. The pits were round depressions usually under 0.1 mm diam, with the majority less than 0.025 mm across. During the formation of these pits, it appears that no material was removed from the surface. For the incubation zone, the rate of damage accumulation is a constant for a given flow condition. Using an annealed 1100 aluminum test probe, a sufficient damage sample could be obtained in a relatively short period of time.

It was observed that the velocity has a marked effect upon the rate of damage production. For a velocity range from 14.9 to 59.3 m/sec, the damage rate increased by approximately the sixth power of velocity. The velocity also affected the sizes of the individual damage pits. The average volume of the pits increased by the fifth power of velocity. The volume of each pit is a measure of the energy required to form it so that the average collapse energy absorbed increases to the fifth power of velocity. A relationship between the pit volume and the absorbed collapse energy was obtained by performing a dynamic hardness test on the model material. Since the pitting rate increases by the sixth power of velocity and the average collapse energy absorbed per pit increases by the fifth power, the total collapse energy absorbed by the model per unit area per second increases by the eleventh power. The pit volume is a measure of the bubble collapse energy absorbed; therefore, a plot of the volume distribution for a given flow condition is also a plot of the bubble collapse energy distribution. Such a plot was generated to show the partition of collapse energies for three flow conditions.

It was observed that the air content and dimensionless cavity length also affected the damage. For a doubling of the air content from 10 to 20 ppm, the rate of damage production was cut nearly in half. There was almost no damage to the models for a very short cavity length. As the length increased, the damage did also. The damage reached a peak and then slowly dropped off for longer cavities.

From high-speed movies of the cavity behavior, it was seen that the cavity regularly breaks off from the model surface. This is due to a re-entrant jet moving through the cavity and striking the leading edge of the cavity. On many of the models, pitting was observed near the leading edge. It is felt that this could be a result of the re-entrant jet behavior. When the jet strikes the cavity wall, it creates a short-term pressure rise, causing any small cavitation bubbles in that area to collapse. If the collapsing bubbles are near the model surface, damage to the model could occur.

In general, good correlation of data was found when a comparison was made with the results of other investigations. The sixth power damage rate law and the actual damage rates involved showed good agreement with three other investigations. The interesting feature of this comparison is the fact that, even though the size and shape of the models used in each of the four investigations were significantly different, the recorded damage rates were approximately the same on an equal velocity basis.

Acknowledgments

The investigation was conducted at the Garfield Thomas Water Tunnel of the Applied Research Laboratory at The Pennsylvania State University under the sponsorship of E/F Research Project 6114. The authors wish to acknowledge the helpful suggestions of M. T. Pigott, who was the monitor of this grant for the sponsor.

References

[1]Thiruvengadam, A., "A Comparative Evaluation of Cavitation Damage Test Devices," Hydronautics, Inc., TR 233-2, 1964.

[2]Knapp, R. T., "Recent Investigations of Cavitation and Cavitation Damage," *Transactions of the American Society of Mechanical Engineers*, Vol. 77, Oct. 1955, pp. 1045-1054.

[3]Tabor, D., *The Hardness of Metals*, Oxford, London, 1951, pp. 115-140.

[4]Hackworth, J. V. and Arndt, R. E. A., "Preliminary Investigations of the Scale Effects of Cavitation Erosion in a Flowing Media," *1974 Cavitation and Polyphase Flow Forum*, American Society of Mechanical Engineers, 1974.

[5]Sato, R., Kato, H., and Tamiya, S., "Study on Cavitation Erosion," *Journal of the Society of Naval Architects, Japan*, Nov. 1973, pp. 43-63 (in Japanese).